

sample calculations above, the fractional disorder required at each position to produce a particular loss of intensity is not a very strong function of the power dependence assumed in eq 1, for values of p close to 1 that occur in slightly disordered phases.

From a biological perspective, the current results suggest that membranes with high levels of cholesterol, such as mammalian cells, may contain more conformational order than might be anticipated from the original fluid mosaic model of membrane structure.²⁷ We are currently examining native membranes enriched in a single acyl chain length to quantitatively explore this hypothesis.

(27) Singer, S. J.; Nicolson, G. L. *Science* 1972, 175, 720.

Finally, previous experiments from this laboratory¹³⁻¹⁵ have introduced spectral parameters for the study of conformational disorder in phospholipid liquid crystalline phases. The CD₂ rocking modes of specifically deuterated acyl chains provide a depth-dependent probe of trans-gauche isomerization, especially in the L_α phase. However, in ordered phases, the bands that reveal gauche rotamer formation are extremely weak and yield band intensities of low precision. The approach presented in the current investigation thus complements the earlier studies and permits a more detailed evaluation of the whole range of conformational order available to hydrocarbon chains.

Acknowledgment. This work was supported by PHS Grant (GM 29864) to R.M.

Mechanism of Antioxidant Reaction of Vitamin E. Charge Transfer and Tunneling Effect in Proton-Transfer Reaction

Shin-ichi Nagaoka,^{*,†} Aya Kuranaka,[†] Hideki Tsuboi,[†] Umpei Nagashima,[†] and Kazuo Mukai^{*,†}

Department of Chemistry, Faculty of Science, Ehime University, Matsuyama 790, Japan, and Institute for Molecular Science, Myodaiji, Okazaki 444, Japan (Received: November 11, 1991)

In order to shed light on the mechanism of proton-transfer reactions, a kinetic and ab initio study of the antioxidant action (intermolecular proton transfer) of vitamin E derivatives has been carried out. The second-order rate constants (k_s 's) for the reaction of tocopherols (TocH's) with variously substituted phenoxy radicals (PhO's) in ethanol were measured with a stopped-flow spectrophotometer. The half-wave reduction potentials ($E_{1/2}$'s) of PhO's were obtained by using a cyclic voltammetry technique. The result indicates that k_s increases as the total electron-donating capacity of the alkyl substituents at the aromatic ring of TocH or the electron-withdrawing capacity of the substituent of PhO increases. k_s for the reaction of deuterated tocopherol derivatives (TocD's) with a PhO in deuterated ethanol (C₂H₅OD, ethanol-*d*₁) was also measured. A substantial deuterium kinetic isotope effect on k_s is observed. In the reactions of each PhO with various TocH's, a plot of log k_s vs peak oxidation potential (E_p) of TocH is found to be linear. The slope of its plot for TocD's is close to that for TocH's. In the reactions of each TocH with various PhO's, a plot of log k_s vs $E_{1/2}$ of PhO is found to be linear. The geometries of TocH's were optimized with the semiempirical modified neglect of diatomic overlap (MNDO) method. The Koopmans' theorem first ionization energies (IP) for those geometries were calculated with the ab initio method. In the reactions of a PhO with various TocH's, plots of log k_s vs IP, the activation energy (E_{act}) vs IP, and E_p vs IP are also found to be linear. From these results, it is considered that both the charge transfer and the proton tunneling play important roles in the antioxidant reaction of TocH. The transition state has the property of the charge-transfer species. The proton tunneling takes place below the transition state. Tunneling allows the proton to cut a corner on the potential energy surface. Our explanation will be widely applicable to many proton-transfer reactions.

Introduction

In recent years, proton transfer has been a topic of much interest because of its importance in many chemical and biological processes.¹⁻⁴ It is a chemically very simple process, which is readily accessible to both accurate measurements and quantitative theoretical analyses. However, the details of the reaction mechanism have not necessarily been elucidated so far. It would be especially interesting to study the tunneling effect. Thus, we have carried out a kinetic and ab initio study to shed light on the mechanism of proton-transfer reactions. As a representative of the proton-transfer reaction, we have chosen the antioxidant action of vitamin E derivatives.

It is well-known that vitamin E (α -, β -, γ -, and δ -tocopherols, Figure 1) inhibits the autoxidation of organic molecules, and the reaction has been studied extensively by numerous investigators.⁵⁻⁸ Furthermore, vitamin E is present in cellular membranes and edible oils and acts as an antioxidant by protecting polyunsaturated lipids or fatty acids from peroxidation.

The antioxidant properties of tocopherols (TocH's) have been ascribed to intermolecular proton transfer (hydrogen transfer)

in the ground state as a whole. The proton (hydrogen) transfers from the OH group in TocH's to a peroxy radical (LOO[•]). The proton transfer (hydrogen transfer) produces a tocopheroxy radical (Toc[•]), which combines with another peroxy radical (reactions 1 and 2).^{9,10}



(1) *Proton-Transfer Reactions*; Caldin, E., Gold, V., Eds.; Chapman and Hall: London, 1975.

(2) *Spectroscopy and Dynamics of Elementary Proton Transfers in Polyatomic Systems*; Barbara, P. F., Trommsdorff, H. P., Eds. *Chem. Phys.* 1989, 136, 153-360.

(3) Nagaoka, S.; Nagashima, U. *Chem. Phys.* 1989, 136, 153.

(4) Nagaoka, S. *Kagaku To Kogyo (Tokyo)* 1991, 44, 182.

(5) Burton, G. W.; Ingold, K. U. *Acc. Chem. Res.* 1986, 19, 194, and references cited therein.

(6) Niki, E. *Yuki Gosei Kagaku Kyokaiishi* 1989, 47, 902, and references cited therein.

(7) Barclay, L. R. C.; Baskin, K. A.; Locke, S. J.; Vinqvist, M. R. *Can. J. Chem.* 1989, 67, 1366.

(8) Pryor, W. A.; Strickland, T.; Church, D. F. *J. Am. Chem. Soc.* 1988, 110, 2224.

(9) Burton, G. W.; Ingold, K. U. *J. Am. Chem. Soc.* 1981, 103, 6472.

(10) Niki, E.; Kawakami, A.; Saito, M.; Yamamoto, Y.; Tsuchiya, J.; Kamiya, Y. *J. Biol. Chem.* 1985, 260, 2191.

[†] Ehime University.

^{*} Institute for Molecular Science. Current address: Department of Computational Science, Faculty of Science, Ochanomizu University, Otsuka, Bunkyo-ku, Tokyo 112, Japan.

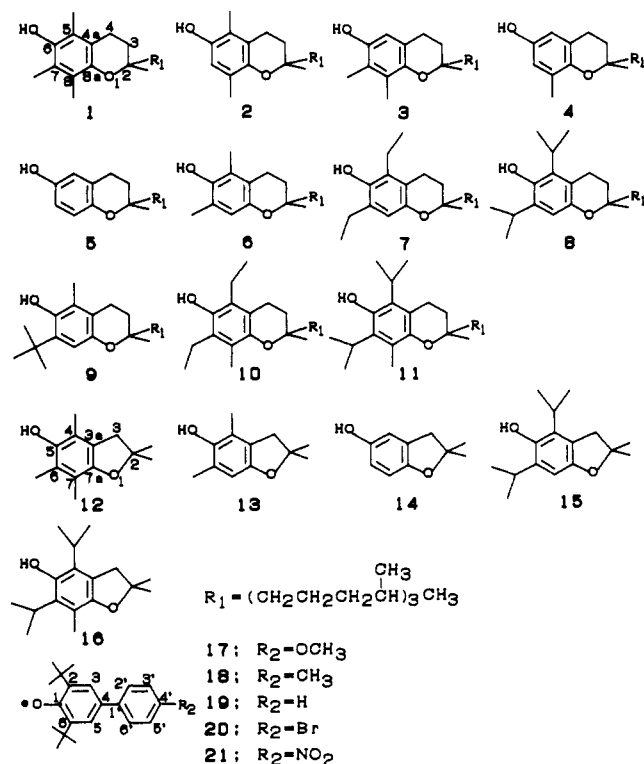


Figure 1. Molecular structures and numbering system for the atoms of TocH's and PhO's.

Here, LOOH stands for a peroxide.

Recently, we¹¹⁻¹⁶ measured the second-order rate constants of TocH's with a stable substituted phenoxyl radical [2,6-di-*tert*-butyl-4-(4'-methoxyphenyl)phenoxy], k_s 's, with a stopped-flow spectrophotometer. We also obtained the peak oxidation potentials (E_p 's)^{17,18} of TocH's by using a cyclic voltammetry technique. The results indicate that k_s increases as the total electron-donating capacity of the alkyl substituents at the aromatic ring of TocH increases. $\log k_s$ was found to correlate with the sum of the Hammett σ constants for all the substituents at the aromatic ring of TocH. It also correlates with the sum of the Brown σ^+ constants and E_p of TocH. The same correlation was found for reaction 1. From these results, we suggested that the antioxidant activity of TocH in reaction 1 depends on the facility of electron transfer from TocH to LOO^{*}; the transition state in reaction 1 has the property of the charge-transfer species. We considered that the mechanism of reactions 1 and 3 can be explained in terms of the electron transfer from TocH to PhO^{*} (or LOO^{*}) followed by the proton transfer from TocH⁺ to PhO^{•-} (or LOO^{•-}). Furthermore, k_s was found to correlate with the rate constant of ¹O₂ removal by TocH.¹⁹ The reaction of ¹O₂ with phenols is known as a charge-transfer reaction.^{20,21} This fact also supports our view

that the charge transfer plays an important role in reaction 1.

On the other hand, Burton et al.²² determined k_1 (reaction 1) by the inhibited autoxidation of styrene method and found that a substantial deuterium kinetic isotope effect on k_1 is observed. From this result, they suggested that the direct hydrogen atom transfer from TocH to LOO^{*} is rate controlling in the antioxidant reaction of TocH.

As mentioned above, two research groups have suggested two different mechanisms, respectively, that play major roles in the antioxidant reaction of TocH: the electron transfer from TocH to LOO^{*} and the direct hydrogen atom transfer from TocH to LOO^{*}. In the present study, we have made a kinetic and ab initio study of the antioxidant reaction of TocH's in order to clarify its mechanism. k_s 's for the reactions of TocH's with variously substituted phenoxyl radicals (PhO^{*}s) in ethanol and the half-wave reduction potentials ($E_{1/2}$'s) of PhO^{*}'s were measured. k_s 's for the reactions of deuterated tocopherols (TocD's) with a substituted phenoxyl radical [2,6-di-*tert*-butyl-4-(4'-methoxyphenyl)phenoxy] in deuterated ethanol (C₂H₅OD, ethanol-*d*₁) were also obtained to examine whether a substantial deuterium kinetic isotope effect on k_s is observed. The geometries of TocH's were optimized with the semiempirical modified neglect of diatomic overlap (MNDO) method. It is interesting to elucidate the relationship between the antioxidant activity and the molecular structure of TocH.

Although E_p depends on the temperature, the solvent, and so on, the ionization energy obtained in the vapor phase by means of HeI photoelectron spectroscopy does not depend on the experimental conditions. It is an inherent value in individual molecules and directly reflects the valence electronic structure of the molecule. However, it is difficult to obtain the ionization energies of TocH's by means of photoelectron spectroscopy.²³ Accordingly, we calculated the Koopmans' theorem first ionization energies (IP) of various TocH's with the ab initio method. It is interesting to elucidate the relationship between the antioxidant activity and the electronic structure of TocH. In fact, the combination of spectroscopy and the ab initio method was a powerful means of investigating the prooxidant reaction of TocH's.²⁴

From these experimental and calculated results, the mechanism of the antioxidant reaction of TocH is discussed in the present paper. In Figure 1 we give the structures of the molecules studied in this work.

Experimental Section

Sample Preparation. *d*- α -, *d*- β -, *d*- γ -, and *d*- δ -tocopherols (1-4, respectively) were kindly supplied from Eisai Co., Ltd. and were used without further purification. Preparation of *dl*-tocol (5) and 2,6-di-*tert*-butyl-4-(4'-methoxyphenyl)phenoxy (17) was reported in a previous paper.¹⁵ 2,6-Di-*tert*-butyl-4-(4'-methylphenyl)phenoxy (18), 2,6-di-*tert*-butyl-4-phenylphenoxy (19), and 2,6-di-*tert*-butyl-4-(4'-bromophenyl)phenoxy (20) were prepared according to the method reported previously.²⁵⁻²⁷ 2,6-Di-*tert*-butyl-4-(4'-nitrophenyl)phenol was synthesized according to the procedure used by Wright and Jorgensen.²⁸ 2,6-Di-*tert*-butyl-4-(4'-nitrophenyl)phenoxy (21) was prepared by the PbO₂ oxidation of 2,6-di-*tert*-butyl-4-(4'-nitrophenyl)phenol in ethanol under a nitrogen atmosphere. Ethanol-*d*₀ (C₂H₅OH) was obtained from Nihon Alcohol and was purified by distillation.

When TocH is dissolved in ethanol-*d*₁ (C₂H₅OD), replacement of the hydrogen atom of the OH group of TocH by a deuterium is easily accomplished. It was verified by proton NMR. Ethanol-*d*₁ of 99.5% purity was purchased from Aldrich and was used without further purification.

(11) Mukai, K.; Watanabe, Y.; Uemoto, Y.; Ishizu, K. *Bull. Chem. Soc. Jpn.* **1986**, *59*, 3113.

(12) Mukai, K.; Yokoyama, S.; Fukuda, K.; Uemoto, Y. *Bull. Chem. Soc. Jpn.* **1987**, *60*, 2163.

(13) Mukai, K.; Fukuda, K.; Ishizu, K. *Chem. Phys. Lipids* **1988**, *46*, 31.

(14) Mukai, K.; Fukuda, K.; Tajima, K.; Ishizu, K. *J. Org. Chem.* **1988**, *53*, 430.

(15) Mukai, K.; Kageyama, Y.; Ishida, T.; Fukuda, K. *J. Org. Chem.* **1989**, *54*, 552.

(16) Mukai, K.; Okabe, K.; Hosose, H. *J. Org. Chem.* **1989**, *54*, 557.

(17) In refs 11-16, the phrase "half-peak oxidation potential" and the symbol $E_{p/2}$ should be replaced by "peak oxidation potential" and E_p , respectively.¹⁸ The peak potential is linearly related to the half-wave potential.¹⁸

(18) *Shin Jikken Kagaku Kouza 5 Kiso Gijyutsu 4 Denki*; Nihon Kagaku Kai, Ed.; Maruzen: Tokyo, 1976. *Shin Jikken Kagaku Kouza 9 Bunseki Kagaku II*; Nihon Kagaku Kai, Ed.; Maruzen: Tokyo, 1977. *Bunseki Kagaku Jikken Handbook*; Nihon Bunseki Kagaku Kai, Ed.; Maruzen: Tokyo, 1987. Osaka, T.; Oyama, N.; Ohsaka, T. *Denki Kagaku Hou—Kiso Sokutei Manual*; Koudansha Scientific: Tokyo, 1989. Matsuda, H.; Ayabe, Y. *Z. Electrochem.* **1955**, *59*, 494.

(19) Mukai, K.; Daifuku, K.; Okabe, K.; Tanigaki, T.; Inoue, K. *J. Org. Chem.* **1991**, *56*, 4188.

(20) Thomas, M. J.; Foote, C. S. *Photochem. Photobiol.* **1978**, *27*, 683.

(21) Saito, I.; Matsuura, T.; Inoue, K. *J. Am. Chem. Soc.* **1983**, *105*, 3200.

(22) Burton, G. W.; Doba, T.; Gabe, E. J.; Hughes, L.; Lee, F. L.; Prasad, L.; Ingold, K. U. *J. Am. Chem. Soc.* **1985**, *107*, 7053.

(23) Katsumata, S., private communication.

(24) Nagaoka, S.; Okauchi, Y.; Urano, S.; Nagashima, U.; Mukai, K. *J. Am. Chem. Soc.* **1990**, *112*, 8921.

(25) Müller, E.; Schick, A.; Scheffler, K. *Chem. Ber.* **1959**, *92*, 474.

(26) Rieker, A.; Ziemek, P. *Z. Naturforsch.* **1965**, *20B*, 640.

(27) Rieker, A.; Scheffler, K. *Justus Liebigs Ann. Chem.* **1965**, *689*, 78.

(28) Wright, J.; Jorgensen, E. C. *J. Org. Chem.* **1968**, *33*, 1245.

TABLE I: k_s and E_{act}^{15} for the Reaction of TocH 1–5 with PhO• 17–21, $E_p^{14,15}$ of TocH 1–5, and $E_{1/2}$ and $\sigma_{PhO\cdot}$ of PhO• 17–21

tocopherols	$10^{-3}k_s, ^a M^{-1} s^{-1}$					E_p vs SCE, mV	E_{act} , kJ/mol
	17 ¹¹	18	19	20	21		
α -TocH (1)	5.12	7.21	8.80	10.8	21.7	860	18.7
β -TocH (2)	2.24	3.98	4.32	6.07	13.2	920	21.1
γ -TocH (3)	2.42	3.56	3.79	5.25	10.7	930	22.2
δ -TocH (4)	1.00	1.62	1.87	3.02	6.21	990	25.6
tocol (5)	0.56	0.67	1.11	1.28	2.27	1050	27.1
$E_{1/2}$ vs SCE, ^b mV	-290 (-284) ²⁹	-240	-200 (-209) ²⁹	-170	-30		
$\sigma_{PhO\cdot}$	-0.27	-0.17	0	0.23	0.78		

^a Experimental errors $\leq \pm 5\%$. ^b Experimental errors $\leq \pm 10$ mV. The peak reduction potentials of 17–21 are estimated to be -360, -300, -280, -220, and -110 mV, respectively.

Measurements. The setup and the experimental procedures for the measurements of the rate constants were described in detail elsewhere.¹⁵ Briefly, the kinetic data were obtained with a Unisoku stopped-flow spectrophotometer Model RS-450 by mixing equal volumes of ethanol solutions of a TocH (1–5) and a PhO• (17–21) under a nitrogen atmosphere. All the measurements were performed at 25.0 ± 0.5 °C.

The pseudo-first-order rate constant for reaction 3 (k_{obsd}) was determined by following a decrease in absorbance of PhO• (for example, at 377 nm in 17).



Here, PhOH stands for a phenol derivative. The rate constant k_{obsd} is given by eq 4. k_0 denotes the rate constant for natural

$$k_{obsd} = k_0 + k_s[TocH] \quad (4)$$

decay of PhO•. k_s stands for the second-order rate constant for the reaction of TocH with PhO•. [TocH] refers to the molar concentration of TocH. These rate parameters were obtained by plotting k_{obsd} against [TocH].

The half-wave reduction potentials ($E_{1/2}$) of 17–21 were obtained by means of cyclic voltammetry. Cyclic voltammetry was performed at room temperature under an atmosphere of nitrogen with a Yanaco cyclic voltammetric analyzer, Model P-1000H. The electrodes used were a platinum electrode and a saturated calomel reference electrode (SCE) in acetonitrile (dried over P_2O_5) containing 40 mM tetrabutylammonium perchlorate. Under these conditions, ferrocene as a standard sample has a half-wave oxidation potential of +400 mV.

Experimental Results

Figure 2 shows the cyclic voltammogram of 21. Similar cyclic voltammograms can also be obtained for 17–20. $E_{1/2}$'s obtained for 17 and 19 are in good agreement with those reported previously.²⁹

k_s 's for the reactions of 1–5 with 17–21 are listed in Table I. E_p 's of 1–5,^{14,15} the activation energies (E_{act} 's) for the reactions of TocH's with 17,¹⁵ $E_{1/2}$ of 17–21, and the Hammett σ constants of the para position for the substituent at the 4'-position of 17–21 ($\sigma_{PhO\cdot}$) are also given in Table I. The substituent at the 4'-position of PhO• will have an influence on the 4-position through the phenyl ring. k_s increases as the total electron-donating capacity of the alkyl substituents at the aromatic ring of TocH or the electron-withdrawing capacity of the substituent of PhO• increases.

Figures 3–5 show plots of $\log k_s$ vs E_p of TocH, $\log k_s$ vs $E_{1/2}$ of PhO•, and $\log k_s$ vs $\sigma_{PhO\cdot}$, respectively. In Figure 3, the plot for each PhO• is found to be linear and the slopes are close to one another. In Figures 4 and 5, the plots for each TocH indicate linear relationships and the slopes in each figure are close to one another. It is clearly more than coincidental that the above-mentioned values cluster near the straight line throughout the various systems studied.

k_s 's for the reactions of deuterated tocopherol derivatives (TocD's) with 17 are listed in Table II, together with the ratios

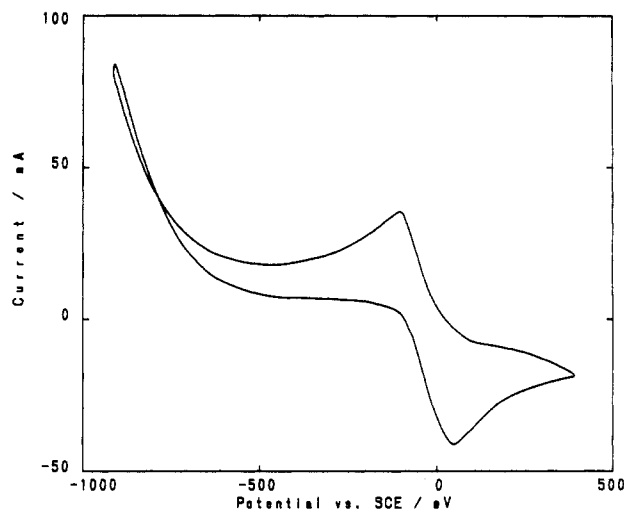


Figure 2. Cyclic voltammogram of 21. The positive and negative directions of the vertical axis correspond to the directions of the increases of the cathodic and anodic currents, respectively.

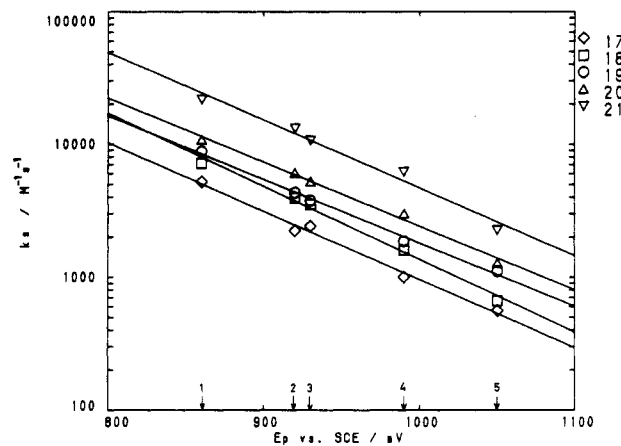


Figure 3. Plot of $\log k_s$ vs E_p of TocH. Arrows 1–5 indicate the positions of E_p 's of 1–5, respectively. The plots for 17–21 give good linear fits with slopes of -5.10, -5.49, -4.77, -4.81, and -5.10 V^{-1} , intercepts of 8.09, 8.62, 8.03, 8.19, and 8.77, and correlation coefficients of 0.995, 0.996, 0.998, 0.996, and 0.989, respectively.

TABLE II: k_s for the Reaction of TocD 1–5 with PhO• 17 and k_s^H/k_s^D

tocopherols	$10^{-2}k_s, ^a M^{-1} s^{-1}$	k_s^H/k_s^D
α -TocD (1)	2.24	22.9
β -TocD (2)	1.49	15.0
γ -TocD (3)	1.61	15.0
δ -TocD (4)	0.642	15.6
tocol- <i>d</i> ₁ (5)	0.305	18.4

^a Experimental errors $\leq \pm 5\%$.

of k_s 's of TocH's to those of TocD's (k_s^H/k_s^D 's). A substantial kinetic isotope effect on k_s is observed. Figure 6 shows plots of

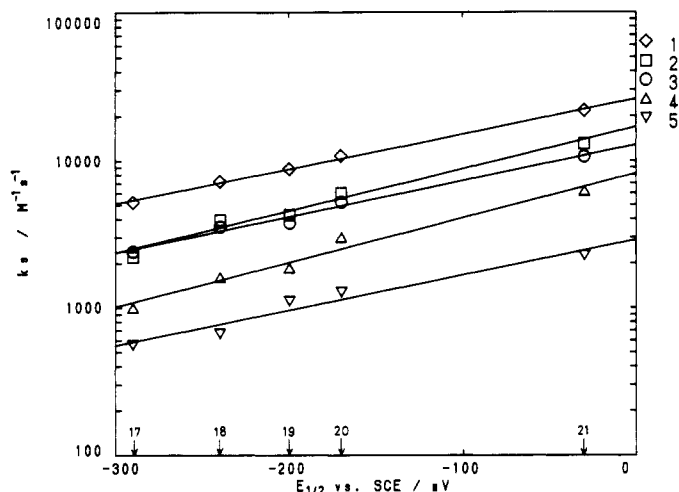


Figure 4. Plot of $\log k_s$ vs $E_{1/2}$ of PhO^\bullet . Arrows 17–21 indicate the positions of $E_{1/2}$'s of 17–21, respectively. The plots for 1–5 give good linear fits with slopes of 2.38, 2.85, 2.45, 3.02, and 2.39 V^{-1} , intercepts of 4.42, 4.23, 4.11, 3.91, and 3.46, and correlation coefficients of 0.998, 0.987, 0.992, 0.985, and 0.974, respectively.

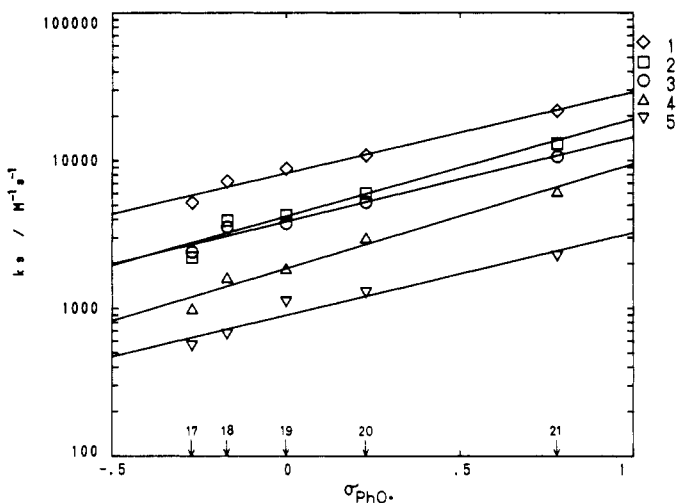


Figure 5. Plot of $\log k_s$ vs $\sigma_{\text{PhO}^\bullet}$. Arrows 17–21 indicate the positions of $\sigma_{\text{PhO}^\bullet}$'s of 17–21, respectively. The plots for 1–5 give good linear fits with slopes of 0.553, 0.659, 0.572, 0.707, and 0.559, intercepts of 3.91, 3.62, 3.59, 3.27, and 2.95, and correlation coefficients of 0.987, 0.972, 0.987, 0.982, 0.969, respectively.

$\log k_s$ for the reactions of TocH's and TocD's with 17 vs E_p of the TocH (TocD). The E_p of TocD is assumed to be equal to that of the corresponding TocH. As in the case of TocH's,^{14,15} the plot for TocD's indicates a linear relationship. The slope of the plot for TocD's is close to that for TocH's. The intercept for TocD's is smaller than that for TocH's.

Calculation Method and Procedure

It is difficult to optimize all the geometries of 1–16 with the ab initio method owing to computer time constraints. Accordingly, the geometries of TocH's have been optimized with the semi-empirical MNDO method. The Koopmans' theorem first ionization energies (IP) for those geometries have been calculated with the ab initio method. IP is simply equal in magnitude to the orbital energy ($-\epsilon$) of the highest occupied molecular orbital (HOMO) as shown in eq 5. In many fundamental organic

$$\text{IP} = -\epsilon \quad (5)$$

molecules studied previously,³⁰ it is known that there is a good correlation between IP and the first ionization energies obtained

(30) Kimura, K.; Katsumata, S.; Achiba, Y.; Yamazaki, T.; Iwata, S. *Handbook of Hel Photoelectron Spectra of Fundamental Organic Molecules*; Japan Scientific Societies Press/Halsted Press: Tokyo/New York, 1981.

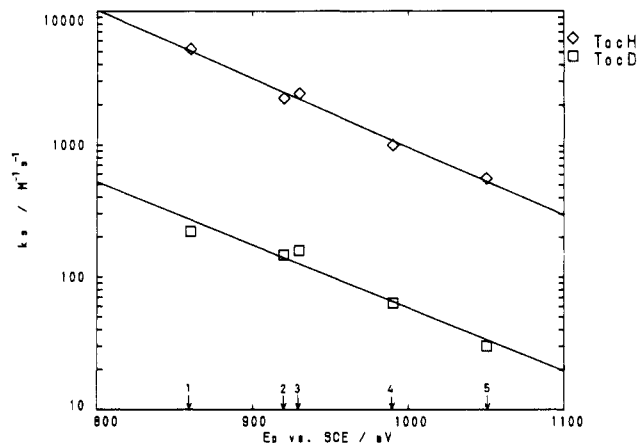


Figure 6. Plots of $\log k_s$ for the reaction of TocH and TocD with 17 vs E_p of the TocH (TocD). Arrows 1–5 indicate the positions of E_p 's of 1–5, respectively. These plots for TocH and TocD give good linear fits with slopes of -5.10 and -4.77 V^{-1} , intercepts of 8.09 and 6.53, and correlation coefficients of 0.995 and 0.979, respectively.

TABLE III: θ and IP for Optimized Geometries of TocH 1–16 in Which the Two Alkyl Groups at the 2-Position Are Replaced by Two Hydrogen Atoms, k_s ,^{11,15,16,35} and E_{act} ^{15,16} for the Reaction of TocH 1–16 with PhO^\bullet 17, and E_p ^{14–16,35} of TocH 1–16

	$\theta, ^\circ$ deg	IP, eV	$10^{-3}k_s, \text{ M}^{-1} \text{ s}^{-1}$	E_p vs SCE, mV	$E_{\text{act}}, \text{ kJ/mol}$
1	18.1	5.23	5.12	860	18.7
2	17.4	5.32	2.24	920	21.1
3	17.0	5.33	2.42	930	22.2
4	17.9	5.43	1.00	990	25.6
5	14.9	5.53	0.56	1050	27.1
6	16.2	5.30	2.39	890	17.5
7	17.5	5.28	1.97	890	18.7
8	18.0	5.29	2.51	890	18.5
9	16.1	5.25	2.97	880	17.8
10	18.0	5.21	3.64	840	
11	15.7	5.14	4.43	860	
12	0.4	5.21	6.99	810	15.8
13	0.0	5.31	3.49	850	17.3
14	0.2	5.53	0.88	1030	28.8
15	0.0	5.30	5.40	870	17.2
16	0.0	5.17	6.49	840	

^a θ denotes the absolute value of the dihedral angle of $\text{C}_{4a}-\text{C}_{8a}-\text{O}_1-\text{C}_2$ in 1–11 or that of $\text{C}_{3a}-\text{C}_{7a}-\text{O}_1-\text{C}_2$ in 12–16.

by means of photoelectron spectroscopy, but the individual values of IP are not in quantitative agreement with the experimental value.

In the present calculation, we replace the two alkyl groups at the 2-position of TocH by two hydrogen atoms to facilitate the calculation. In fact, k_1 of α -TocH is close to that of 6-hydroxy-5,7,8-trimethylchroman.²² Furthermore, in the simple one-electron ejection picture, an electron is ejected from HOMO (π -type) in the first ionic state of TocH. Since the alkyl groups at the 2-position are located far from the aromatic π electron system, substitution of the hydrogen atoms for the alkyl groups may not have a large influence on the IP of TocH.

The MNDO calculations of TocH's were performed with the MOPAC program.³¹ The MNDO calculation reproduces the experimental geometry fairly well.³² Ab initio self-consistent-field (SCF) calculations were carried out with the GAUSSIAN 86 program.³³ The basis set used in the present calculations is STO-3G,

(31) Stewart, J. J. P. *QCPE No. 455*, 1983.

(32) Nagashima, U.; Fujimoto, H.; Inokuchi, H.; Seki, K. *J. Mol. Struct.* **1989**, *197*, 265.

(33) Frisch, M. J.; Binkley, J. S.; Schlegel, H. B.; Raghavachari, K.; Melius, C. F.; Martin, R. L.; Stewart, J. J. P.; Bobrowicz, F. W.; Rohlfing, C. M.; Kahn, L. R.; DeFrees, D. J.; Seeger, R.; Whiteside, R. A.; Fox, D. J.; Fluder, E. M.; Topiol, S.; Pople, J. A. *GAUSSIAN 86*; Carnegie-Mellon Quantum Chemistry Publishing Unit, Carnegie-Mellon University: Pittsburgh, PA, 1986; registered at IMS Program Library by N. Koga, S. Yabushita, K. Sawabe, and K. Morokuma (IMS).

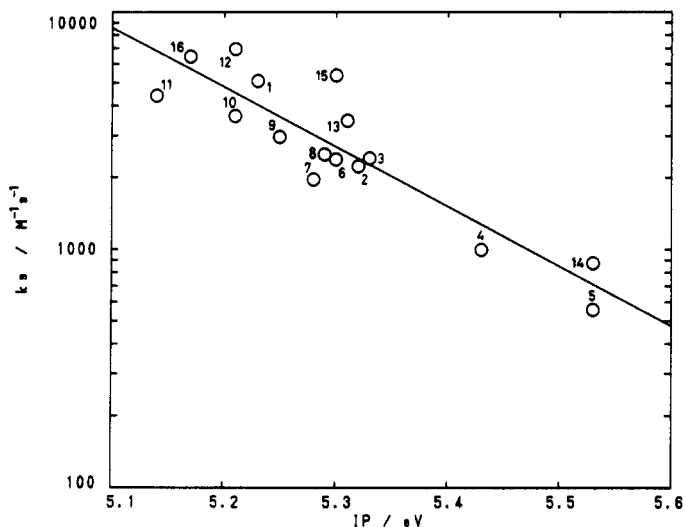


Figure 7. Plot of $\log k_s$ for the reaction of ToCH's (1–16) and 17 vs IP of the ToCH's. This plot gives a linear fit with a slope of -2.51 eV^{-1} , an intercept of 16.7, and a correlation coefficient of 0.900.

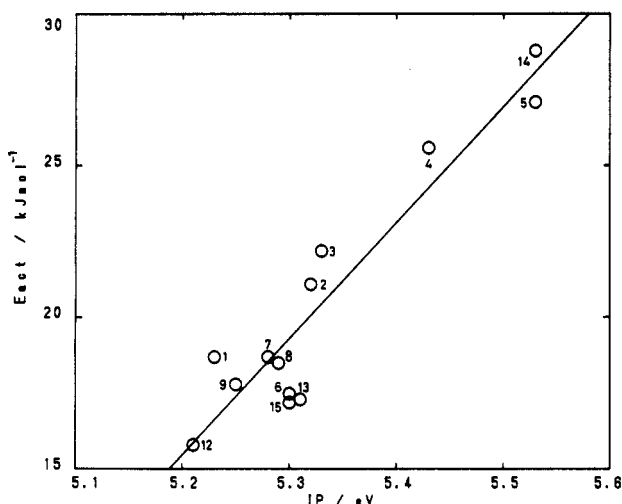


Figure 8. Plot of E_{act} for the reaction of ToCH's (1–9 and 12–15) vs IP of the ToCH's. This plot gives a linear fit with a slope of $38.3 \text{ kJ/mol}\cdot\text{eV}$, an intercept of -184 kJ/mol , and a correlation coefficient of 0.938.

which has been thoroughly tested on organic molecules and reproduces the experimental results fairly well.³⁴ Numerical calculations were carried out at the Computer Center of Institute for Molecular Science (IMS).

Calculated Results

Optimized geometries of 1–16 are available as supplementary material. The dihedral angle between the 2p-type lone pair on O_1 and the π orbital of the adjacent aromatic carbon (θ) and IP obtained are listed in Table III. θ is equal to the absolute value of the dihedral angle of $C_{4a}-C_{8a}-O_1-C_2$ in 1–11 or that of $C_{3a}-C_{7a}-O_1-C_2$ in 12–16. The experimental results of E_p ^{14–16,35} of ToCH's, k_s ^{11,15,16,35} and the activation energy (E_{act})^{15,16} for the reaction of ToCH's with 17 are also given in Table III. It is shown that the smaller the IP of ToCH, the larger the k_s and the smaller the E_p and E_{act} . Such relation among IP, E_p , k_s , and E_{act} is generally found throughout the various ToCH's studied.

Figures 7–9 show plots of $\log k_s$ vs IP of the ToCH's, E_{act} vs IP of the ToCH's, and E_p vs IP in ToCH's, respectively. These plots are found to be linear. It is clearly more than coincidental that the above-mentioned values cluster near the straight line throughout the various systems studied.

(34) Hehre, W. J.; Radom, L.; Schleyer, P. v. R.; Pople, J. A. *Ab Initio Molecular Orbital Theory*; John Wiley & Sons: New York, 1986.

(35) Mukai, K., unpublished data.

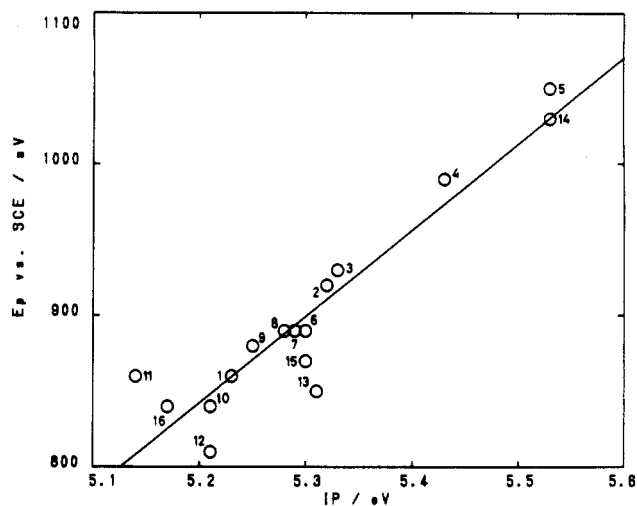


Figure 9. Plot of E_p vs IP in ToCH's (1–16). This plot gives a linear fit with a slope of $5.70 \times 10^2 \text{ mV/eV}$, an intercept of -2.12 V , and a correlation coefficient of 0.932.

The five-membered heterocyclic rings of 12–16 are more planar than the six-membered rings of 1–11 and θ 's of the 12–16 are smaller than those of 1–11.

Mechanism of Antioxidant Reaction of ToCH

The elucidation of reaction mechanisms is a major challenge in the present study. On the basis of the experimental and calculated results mentioned above, we will try to explain the mechanism of the antioxidant action of ToCH in this section.

k_s depends on the electron-donating and electron-withdrawing properties of the substituents on the ToCH and PhO^* , respectively. Furthermore, straight-line relationships can be seen in Figures 3–5. From these results, it is considered that the electron transfer from ToCH to LOO^* (or PhO^*) plays an important role in reactions 1 and 3. This electron transfer will correspond to the "normal region" in Marcus theory³⁶ and/or the Rehm–Weller equation.³⁷

The straight-line relationship shown in Figures 3 and 4 can be expressed mathematically by

$$\log k_s = -C_1 E_p + C_2 \quad (6)$$

$$\log k_s = C_3 E_{1/2} + C_4 \quad (7)$$

respectively, where C_1 – C_4 are constants. The relation between k_s and E_{act} can be expressed mathematically by¹⁵

$$\log k_s = -C_5 E_{\text{act}} + C_6 \quad (8)$$

where C_5 and C_6 are constants. From eqs 6–8, it is suggested that E_{act} includes the terms of the energy required to eject an electron from ToCH and the energy released in the acceptance of an electron by PhO^* . In fact, there is a good correlation between E_{act} and E_p of ToCH, as reported previously.¹⁵ Accordingly, the transition state in reactions 1 and 3 is considered to have the property of the charge-transfer species such as $\text{LOO}^{\cdot\cdot\cdot}\text{ToCH}^+$ (reaction 1) or $\text{PhO}^{\cdot\cdot\cdot}\text{ToCH}^+$ (reaction 3).

From Table III, it is shown that the smaller the IP, the larger the k_s and the smaller the E_{act} . Furthermore, the plots of $\log k_s$ vs IP of ToCH and E_{act} vs IP of ToCH indicate good linear relationships as shown in Figures 7 and 8, respectively. These facts also support our view that the electron transfer from ToCH to PhO^*

(36) Marcus, R. A. *J. Chem. Phys.* **1956**, *24*, 966; *Annu. Rev. Phys. Chem.* **1964**, *15*, 155. Marcus, R. A.; Sutin, N. *Biochim. Biophys. Acta* **1985**, *811*, 265. *Kikan Kagaku Sosetsu, Yuki Denshi Idou Process*; Nihon Kagaku Kai, Ed.; Gakkai Shuppan Center: Tokyo, 1988, Chapter 1, and references cited therein.

(37) Rehm, D.; Weller, A. *Ber. Bunsenges. Phys. Chem.* **1969**, *73*, 834; *Isr. J. Chem.* **1970**, *8*, 259. *Kikan Kagaku Sosetsu, Yuki Denshi Idou Process*; Nihon Kagaku Kai, Ed.; Gakkai Shuppan Center: Tokyo, 1988, Chapter 7, and references cited therein.

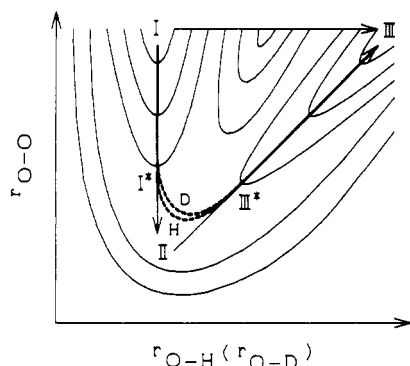


Figure 10. Schematic contour map of potential energy surface in antioxidant reaction of TocH (TocD). The distance between PhO^* (or LOO^*) and TocH (TocD), that is, the distance between the oxygen atom in PhO^* (or LOO^*) and that in the OH (OD) group of TocH or TocD ($r_{\text{O-O}}$), is plotted as ordinate and the O-H (O-D) bond length of TocH ($r_{\text{O-H}}$) or TocD ($r_{\text{O-D}}$) as abscissa. I, I*, II, III*, and III denote the following: I, PhO^* (or LOO^*) + TocH; I*, a partial charge-transfer species $\text{PhO}^{\delta-}\cdots\text{TocH}^{\delta+}$ (or $\text{LOO}^{\delta-}\cdots\text{TocH}^{\delta+}$); II, the charge-transfer species $\text{PhO}^{\cdots}\cdots\text{TocH}^+$ (or $\text{LOO}^{\cdots}\cdots\text{TocH}^+$); III*, $\text{PhOH}\cdots\text{Toc}^*$ (or $\text{LOOH}\cdots\text{Toc}^*$); III, PhOH (or LOOH) + Toc^* . The reaction trajectory corresponding to the electron transfer from TocH to PhO^* (or LOO^*) followed by proton transfer from TocH^+ to PhO^{\cdots} (or LOO^{\cdots}), the direct hydrogen atom transfer, and the real one are represented by I \rightarrow II \rightarrow III, I \rightarrow III (direct path), and a bold-face line (I \rightarrow I* \rightarrow III* \rightarrow III), respectively. The solid and dotted parts of the bold-face line denote the classical and tunneling motions in the real reaction trajectory, respectively. The dotted parts H and D correspond to the tunneling paths for the reactions of TocH and TocD, respectively.

(or LOO^*) plays an important role in reactions 1 and 3. In the simple one-electron-transfer picture, an electron is ejected from the highest occupied molecular orbital (HOMO, π -type) of TocH and is accepted to the singly occupied molecular orbital (SOMO) of PhO^* (or LOO^*) in this electron transfer. The energy of SOMO of PhO^* (or LOO^*) is always larger than that of HOMO of TocH in the present system. As the IP of TocH decreases, the energy of HOMO increases (eq 5) and approaches that of SOMO of PhO^* (or LOO^*). As a result, the facility of the charge transfer from TocH to PhO^* (or LOO^*) increases and the charge-transfer species is stabilized.

As shown in Figure 6, a substantial deuterium kinetic isotope effect on k_s is observed ($k_s^{\text{H}}/k_s^{\text{D}} = 22.9$ in α -TocH). From this result, it is considered that proton tunneling plays an important role in reactions 1 and 3. As the mass of the H (D) atom increases, the zero-point energy of the OH (OD) stretching vibration decreases and the thickness of the potential barrier of the proton-transfer (hydrogen-transfer) reaction increases.^{38,39} The probability of proton tunneling decreases, accompanying an increase in the mass of the H (D) atom and the thickness of the potential barrier.^{38,39} As a result, the substantial deuterium kinetic isotope effect on k_s is considered to be observed. In the antioxidant reaction of TocH, the proton tunneling manifests itself in $k_s^{\text{H}}/k_s^{\text{D}}$ determined here.

On the basis of the experimental and calculated results mentioned above, we offer a probable explanation for the mechanism of the antioxidant reaction of TocH. Figure 10 shows a schematic contour map of the potential energy surface in the antioxidant reaction of TocH (TocD). The distance between PhO^* (or LOO^*) and TocH (TocD), that is, the distance between the oxygen atom in PhO^* (or LOO^*) and that in the OH (OD) group of TocH or TocD ($r_{\text{O-O}}$), is plotted as ordinate and the O-H (O-D) bond length of TocH ($r_{\text{O-H}}$) or TocD ($r_{\text{O-D}}$) as abscissa. I, I*, II, III*, and III denote the following: I, PhO^* (or LOO^*) + TocH; I*, a partial charge-transfer species ($\text{PhO}^{\delta-}\cdots\text{TocH}^{\delta+}$ or $\text{LOO}^{\delta-}\cdots\text{TocH}^{\delta+}$); II, the charge-transfer species $\text{PhO}^{\cdots}\cdots\text{TocH}^+$ (or

$\text{LOO}^{\cdots}\cdots\text{TocH}^+$); III*, $\text{PhOH}\cdots\text{Toc}^*$ (or $\text{LOOH}\cdots\text{Toc}^*$); III, PhOH (or LOOH) + Toc^* .

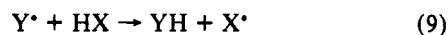
Previously, we considered that the mechanism of reactions 1 and 3 could be explained in terms of the electron transfer from TocH to PhO^* or LOO^* followed by the proton transfer from TocH^+ to PhO^{\cdots} or LOO^{\cdots} (I \rightarrow II \rightarrow III).¹¹⁻¹⁶ To the contrary, Burton et al. considered that the direct hydrogen atom transfer from TocH to PhO^* (or LOO^*) is rate controlling in reaction 1;²² that is, the reaction trajectory corresponds to the direct one from I to III. However, the real typical reaction trajectory can be represented by a bold-face line in Figure 10. The solid and dotted parts of the bold-face line denote the classical and tunneling motions in the reaction trajectory, respectively. The dotted parts H and D correspond to the tunneling paths for the reactions of TocH and TocD, respectively. The tunneling path of TocD is longer than that of TocH.

I and III are separate local energy minima, and each of the possible paths connecting them will have an energy maximum. There is a high and thick potential barrier between I and III. Accordingly, the direct hydrogen atom transfer (direct path from I to III) is not preferred as a path of the antioxidant reaction of TocH in either classical jump or tunneling. The reaction roughly follows, instead, the path along which the energy gradient is minimum.

In the initial stage of the reaction, PhO^* (or LOO^*) and TocH approach each other and their electron clouds begin to overlap (I \rightarrow I*). Then, SOMO of PhO^* (or LOO^*) and HOMO of TocH begin to interact in the simple one-electron-transfer picture. PhO^* (or LOO^*) and TocH are relatively susceptible to accepting and donating an electron, respectively. Thus, the final goal of this process is the transition state (saddle point, the lowest energy maximum in Figure 10) which has the property of the charge-transfer species (II). When PhO^* (or LOO^*) and TocH approach each other to some extent, the proton tunneling takes place below the transition state (the dotted part of the bold-face line in Figure 10, I* \rightarrow III*). Here, I* has the property of a partial charge-transfer species ($\text{PhO}^{\delta-}\cdots\text{TocH}^{\delta+}$ or $\text{LOO}^{\delta-}\cdots\text{TocH}^{\delta+}$). Tunneling allows the proton to cut a corner on the potential energy surface. More or less simultaneous transfer of proton and electron takes place then. Finally, PhOH (or LOOH) and Toc^* separate from each other (III* \rightarrow III).

It is, thus, concluded that both charge transfer and proton tunneling play important roles in the antioxidant reaction of TocH. The charge transfer and the proton tunneling could be different sides of the same coin, and it seems unsound to present them as conflicting models. The above-mentioned mechanism satisfactorily accounts for the antioxidant action of TocH. Our explanation for the antioxidant reaction of vitamin E allows us to recognize its important features very well.

It is interesting to examine whether other proton-transfer (hydrogen-transfer) reactions (reaction 9) can be explained in



terms of the same mechanism. So far, numerous investigators have offered Scheme I or II for the reaction mechanism of reaction 9.

Scheme I: Charge transfer



Scheme II: Direct hydrogen atom transfer

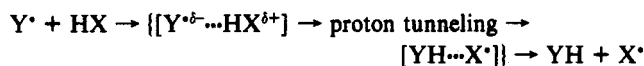


However, Schemes I and II may not be necessarily contradictory. Scheme I is based on kinetic (thermodynamic) grounds, and Scheme II provides an explanation for the deuterium isotope effect. As in the case of the antioxidant reaction of TocH, the two schemes could be different sides of the same coin. The relative weight of each scheme in the observation of reaction 9 is considered to depend on the shape of the potential energy surface in the system. The real total scheme of reaction 9 may be represented by Scheme III.

(38) Atkins, P. W. *Physical Chemistry*; Oxford University Press: London, 1982.

(39) Kuranaka, A.; Sawada, K.; Nagashima, U.; Nagaoka, S.; Mukai, K. *Vitamins* 1991, 65, 453.

Scheme III: Our new explanation



The implication of this paper will be important in various proton-transfer reactions.

Discussion

In Figure 6, the slope of the plot for TocD is close to that for TocH. $k_s^{\text{H}}/k_s^{\text{D}}$ does not change appreciably with the substitution at the aromatic ring of TocH, as shown in Table II. Accordingly, it is considered that the substitution at the aromatic ring does not have a large influence on the probability of proton tunneling. The thickness of the potential barrier and the shape of the potential energy surface around the transition state (saddle point in Figure 10) will not depend largely on the substitution. The substitution is likely to affect E_{act} alone.

In each of Figures 3–5, the slopes of the linear relationships are close to one another. These facts indicate that the substitution effects in TocH and PhO[•] contribute to k_s independently and additively. If this is equally true of reaction 1, we can predict k_1 from the substituents of TocH and LOO[•]. In fact, a plot of $\log k_1$ vs E_p is linear and the slope is similar to those in Figure 3.¹⁴ The results shown here will be useful for future studies concerning protection of polyunsaturated lipids or fatty acids from peroxidation. Because the frequency factors in k_s 's are smaller than those in k_1 's, k_s 's are smaller than k_1 's.

Burton et al.^{22,40–42} explained the difference in antioxidant activity between α -TocH and 4-methoxytetramethylphenol in the following way. The difference is due to the extent of orbital overlap between the 2p-type lone pair on the ring oxygen or the methoxy oxygen and the aromatic π electron system. The high antioxidant activity of α -TocH is attributed to the fact that the 2p-type lone pair of electrons on the ring oxygen lies approximately parallel to the π orbital of the aromatic plane; the α -Toc[•] radical is stabilized by this lone pair, the OH bond is weakened, and in consequence, α -TocH has a large k_1 value. In contrast, since the 4-methoxytetramethylphenoxyl radical is not stabilized by the lone pair, 4-methoxytetramethylphenol has a relatively small k_1 value. The extent of orbital overlap between the 2p-type lone pair on the ring oxygen and the aromatic π electron system in TocH increases as θ decreases. It would be worthwhile to examine whether or not the orbital overlap is a factor governing the antioxidant activity of 1–11.

However, the molecular structures of 2–16 have not been obtained experimentally so far. This problem is serious in the elucidation of the relationship between the molecular structure and the antioxidant activity of TocH. Since there are no experimental molecular structures of 2–16, we have predicted these theoretically (Table III). TocH with a small θ value does not necessarily have a large k_s value in 1–11 (Table III). Thus, at least within the scope of TocH's with a six-membered heterocyclic ring, the orbital overlap is not a dominant factor governing the antioxidant activity.

However, θ 's of TocH's with a five-membered heterocyclic ring (12–16) are smaller than those with a six-membered ring (1–11). k_s increases on going from TocH with a six-membered heterocyclic ring (1, 6, 5, 8, and 11) to the corresponding TocH with a five-membered heterocyclic ring (12, 13, 14, 15, and 16, respectively), as shown in Table III. Accordingly, it is considered that, in those cases, the increase in the extent of orbital overlap between the 2p-type lone pair on the ring oxygen and the aromatic π electron system induces the increase in k_s . Because k_s of 1 is larger than that of 14 (Table III), the electron-donating capacity of the substitution at the aromatic ring of TocH affects k_s more greatly than the orbital overlap.

We have combined two attractive approaches—stopped-flow technique and ab initio calculation. Comparing calculated IP's of TocH's with the experimental values of k_s 's, E_{act} 's, and E_p 's of TocH's, we have found some systematic correlations, which are given in Figures 7–9. Such correlations are expected to be useful in future use of the molecular orbital calculations for predicting those experimental values without experiments. One can adopt the molecular orbital calculation as a tactic for finding new molecules having high antioxidant activities.

We have naturally examined other possibilities for the mechanism of the antioxidant reaction of TocH as well. The experimental results shown in Figures 3–6 are unlikely due to the two competitive processes, that is, the electron transfer followed by the proton transfer (I \rightarrow II \rightarrow III) and the hydrogen tunneling in the direct hydrogen transfer (I \rightarrow III). If such two competitive processes are present, the relative importance of the former decreases and that of the latter increases with decreasing temperature. As a result, an Arrhenius plot of k_s must become nonlinear and k_s must tend to become temperature independent in the low-temperature region. However, our experimental results are evidently not like that.^{15,16} Furthermore, if the above-mentioned two competitive processes are operative, the relative importance of the hydrogen tunneling must decrease and $k_s^{\text{H}}/k_s^{\text{D}}$ must approach unity accompanying a decrease in the activation energy of the electron transfer (E_{act}). However, $k_s^{\text{H}}/k_s^{\text{D}}$ is independent of E_{act} and is much larger than unity (Tables I and II). Thus, in summary, it seems most likely that the real reaction trajectory around room temperature can be represented by the bold-face line shown in Figure 10.

The antioxidant reaction of TocH scavenges LOO[•] and produces Toc[•]. Toc[•] is relatively safe for cellular membranes, because vitamin C reduces Toc[•] back to TocH.^{43–45} On the other hand, the transition state of the antioxidant reaction has the property of the charge-transfer species (LOO^{••-}...TocH^{•+}) in which positive and negative charges must be separated. Such charge separation is very dangerous to cellular membranes, because it may disturb the membrane potential and/or may induce another undesirable side reaction. Accordingly, the proton tunneling takes place below the transition state and the explicit charge separation is avoided during the antioxidant reaction. The tunneling proton accompanies the transferring charge. The antioxidant reaction of TocH in vivo functions skillfully.

Conclusion

In order to shed light on the mechanism of proton-transfer reactions, a kinetic and ab initio study of the antioxidant action (intermolecular proton transfer) of vitamin E derivatives has been carried out. k_s 's for the reactions of TocH's with various PhO[•]'s in ethanol- d_0 were measured with a stopped-flow spectrophotometer. $E_{1/2}$'s of PhO[•]'s were obtained by using a cyclic voltammetry technique. The result indicates that k_s increases as the total electron-donating capacity of the alkyl substituents at the aromatic ring of TocH or the electron-withdrawing capacity of the substituent of PhO[•] increases. k_s for the reaction of TocD's with a PhO[•] in ethanol- d_1 was also measured. A substantial deuterium kinetic isotope effect on k_s is observed. A plot of $\log k_s$ vs E_p of TocH is found to be linear. The slope of its plot for TocD's is close to that for TocH's. A plot of $\log k_s$ vs $E_{1/2}$ of PhO[•] is found to be linear. The geometries of TocH's were optimized with the MNDO method and IP's for those geometries were calculated with the ab initio method. Plots of $\log k_s$ vs IP, E_{act} vs IP, and E_p vs IP are also found to be linear. From these results, it is considered that both the charge transfer and the proton tunneling play important roles in the antioxidant reaction of TocH. The transition state has the property of the charge-transfer species. The proton tunneling takes place below the transition state. Tunneling allows the proton to cut a corner on the potential energy surface. The mechanism of the antioxidant action of TocH can

(40) Burton, G. W.; Le Page, Y.; Gabe, E. J.; Ingold, K. U. *J. Am. Chem. Soc.* **1980**, *102*, 7791.

(41) Burton, G. W.; Hughes, L.; Ingold, K. U. *J. Am. Chem. Soc.* **1983**, *105*, 5950.

(42) Doba, T.; Burton, G. W.; Ingold, K. U. *J. Am. Chem. Soc.* **1983**, *105*, 6505.

(43) Tappel, A. L. *Geriatrics* **1968**, *23*, 96.

(44) Packer, J. E.; Slater, T. F.; Willson, R. L. *Nature* **1979**, *278*, 737.

(45) Mukai, K.; Nishimura, M.; Kikuchi, S. *J. Biol. Chem.* **1991**, *266*, 274.

be explained in terms of Scheme III of reaction 9. The charge transfer and the proton tunneling could be different sides of the same coin, and it seems unsound to present them as conflicting models. Our explanation will be widely applicable to many proton-transfer reactions.

Acknowledgment. We thank Eisai Co. Ltd. for the generous gift of *d*- α -, *d*- β -, *d*- γ -, and *d*- δ -tocopherols. Our thanks are also due to the Computer Center of the Institute for Molecular Science (IMS) for the use of the HITAC M-680H and S-820/80 computer

and the Library Program GAUSSIAN 86³³ and MOPAC.³¹ We also thank Mr. Kouhei Sawada of Ehime University for his kindness in helping A.K. and H.T. in their works and Mr. Shingo Itoh of Ehime University for his valuable discussion concerning the cyclic voltammetry.

Supplementary Material Available: Optimized geometries of 1-16 with the MNDO method (Figures 11-27) and the dihedral angles for 1-11 (Table IV) and 12-16 (Table V) (20 pages). Ordering information is given on any current masthead page.

Neural Network Predictions of Energy Transfer in Macromolecules

Bobby G. Sumpter,* Coral Getino, and Donald W. Noid

Chemistry Division, Oak Ridge National Laboratory, Oak Ridge, Tennessee 37831-6182, and Department of Chemistry, The University of Tennessee, Knoxville, Tennessee 37996-1600 (Received: October 1, 1991; In Final Form: November 18, 1991)

A neural network is trained to predict the dynamical behavior of internal energy in macromolecules. Energy flow out of localized sites within a polyethylene chain is studied as a function of time, excitation level, and temperature. Computations were examined for CH stretch excitation levels between $\nu = 2$ and 14, temperatures between $T = 20$ and 350 K, and time from 0 to 200 ps. The results show that the neural network predictions are accurate to within 8% error of those calculated from molecular dynamics. This difference is related to statistical fluctuations in the molecular dynamics calculations which result from small ensemble averages. In fact, the neural network acts to "filter out" those fluctuations, providing results which are more concordant with the limit of a very large ensemble average. In addition to this desirable property, the trained network can predict energy flow behavior for any reasonable excitation level, temperature (energies must be bound), and time scale, thereby significantly extending the computational limits of the molecular dynamics method.

I. Introduction

With the advent of new state-of-the-art experimental methods to study ultra-fast energy relaxation,¹ there has been considerable interest in extending the present understanding of vibrational energy flow in small polyatomic systems^{1,2} to the study of internal energy flow in macromolecular systems.³⁻⁵ In recent years, the technique of time-resolved vibrational spectroscopy has been used to examine energy relaxation in condensed matter systems and in solids.^{3,4} Graener and Laubereau⁴ were among the first to use this technique to study the vibrational population decay of CH stretching modes in crystalline polyethylene. They excited the infrared active CH stretch vibrations of a polyethylene crystal by using 10-mJ picosecond pulses from a Nd:YAG mode-locked laser. By doubling a small fraction of the fundamental laser pulse, they were able to create a probe pulse which was then used in anti-stokes Raman scattering. Their results indicated that the time delay between the absorption of the initial laser pulse and the population of the Raman active modes was on a time scale of less than 5 ps. A second and much slower time constant (on the order of 260 ps) was also measured and loosely attributed to energy redistribution throughout the crystal (thermalization time). The two different energy redistribution processes lead to the conclusion that the energy randomization in polyethylene could not be described by a single decay constant and that the observed decay must be characterized by a yet unknown subensemble of vibrational modes.

The results on polyethylene have some striking similarities to the energy flow characteristics of polyatomic molecules in the gas-phase. The observation of an initial rapid decay of the excited vibrational modes closely parallels that observed in X-H overtone

decay.^{1,2} In particular, it occurs on a rapid time scale compared to other large scale dynamical processes such as chemical reactions. Energy flow mechanisms for this type of decay are generally a result of nonlinear resonances.² Indeed, Graener and Laubereau⁴ suggested that Fermi resonance could provide a possible coupling for the randomization of energy in crystalline polyethylene.

In order to bring together the experimental results on polyethylene with those of theoretical studies on X-H overtone decay in small polyatomics, we have previously performed a series of very detailed computational experiments.⁵ The energy flow behavior of CH stretches in a single chain of polyethylene and its sensitivity to details such as potential energy surface, CH stretch excitation energy, temperature, and pressure were examined. The rate of energy flow from CH stretching modes was observed to be very rapid and irreversible, occurring on a time scale of less than 0.5 ps at low temperatures and increases with overall increasing temperature. A characteristic two-phase energy flow behavior was observed, where the initial part consisted of a very rapid flow due to the decay of the initial excitation followed by a slower flow due to energy redistribution throughout the system. The mechanism for the initial facile energy flow was found to involve strong CH stretch/HCH bend Fermi (1:2) resonant pathways. The long-time dynamics, associated to complete redistribution of the initial CH stretch energy to all of the available vibrational modes, occurs within a time of 2 ps. A similar two-phase behavior of energy flow was observed for the solid (polymer crystal): while the intramolecular redistribution occurs in a slightly shorter time scale (~ 0.1 ps) than that for a single chain, the long-time component or intermolecular redistribution (in this case related to chain-to-chain energy transfer) is 2 orders of magnitude larger. These results demonstrated for the first time a definite resonance-enhanced mechanism for the intramolecular (about 2 ps) and intermolecular (0.2 ns) energy redistribution in polyethylene crystals.

While the previous study of vibrational energy flow was carried out in great detail, it was nevertheless constrained by computational time. Calculations were carried out in limited regions of the multidimensional phase space and for finite ensemble sizes

(1) Crim, F. F. *Science* 1990, 249, 1387. Zewail, A.; Bernstein, R. B. *Chem. Eng. News* 1988, 66, 24.

(2) For a recent review see: Uzer, T.; Miller, W. H. *Phys. Rep.* 1990, 199, 73.

(3) See papers in: *Chem. Rev.* 1990, 90. *Chem. Phys.* 1990, 146.

(4) Graener, H.; Laubereau, A. *Chem. Phys. Lett.* 1987, 133, 378.

(5) Sumpter, B. G.; Noid, D. W. *Chem. Phys.*, in press.